JOURNAL OF AGRICULTURAL AND FOOD CHEMISTRY

Preparation and Characterization of Inclusion Complex of Iprodione and β-Cyclodextrin to Improve Fungicidal Activity

XIAO-LEI ZHU†, HONG-BO WANG,† QIONG CHEN, WEN-CHAO YANG, AND GUANG-FU YANG*

Key Laboratory of Pesticide & Chemical Biology, Ministry of Education, College of Chemistry, Central China Normal University, Wuhan 430079, People's Republic of China

The effect of β-cyclodextrin (β-CD) on the improvement of the fungicidal activity of iprodione has been investigated. The inclusion complexation of β-CD with iprodione has been prepared and characterized by integrating some analytical techniques (such as electrospray ionization−mass spectrometry, differential scanning calorimetry, thermogravimetry, x-ray diffraction, and scanning eletron microscopy) and molecular simulation methods. The β-CD/iprodione inclusion complex has exhibited different spectroscopic features and properties from iprodione. The stoichiometric ratio and stability constant describing the extent of formation of inclusion complexes have been determined by phase solubility studies. The calculated apparent stability constant of the iprodione/β-CD complex was 407.5 M^{-1}. The obtained inclusion complexes were found to significantly improve the water solubility of iprodione, and there is a 4.7-fold increase in the presence of 13 mM β-CD as compared with the solubility of iprodione in deionized water in the absence of β-CD. The bioassay demonstrated that the complex displayed over two-fold increase of the fungicidal activity. In addition, the possible structure of the β-CD/iprodione complex was proposed according to the results of the molecular dynamic simulation. The present study provided useful information for a more rational application of iprodione, diminishing the use of organic solvents and increasing its efficacy.

KEYWORDS: Cyclodextrins; iprodione; inclusion complex; antifungal activity; molecular modeling

INTRODUCTION

Cyclodextrins (CDs) are a class of natural cyclic oligosaccharides composed of six (α-), seven (β-), or eight (γ-) D-glucopyranose residues linked by α-(1,4)-bonds (*1*). Because of its high molecular recognition ability toward a variety of guest molecules, CDs have been widely used in the pharmaceutical industry with the aim to enhance the water solubility, chemical stability, and bioavailability of insoluble or poorly soluble drugs, to reduce toxicity, and to control the release rate (*2*−*5*). The same effect has been demonstrated with other drugs of interest in the agriculture industry (*6*−*14*).

Iprodione, a dicarboximide fungicide as shown in **Scheme 1**, has been extensively used to control a variety of crop diseases for decades (*16*−*18*). It has been established that iprodione exhibited its fungicidal activity by inhibiting the spores' germination and the mycelia's growth. However, iprodione has a poor water solubility (1.3×10^{-2}g/L) and transportation property. Therefore, significant increases in resistance against iprodione were observed in a range of important plant pathogens after a long-time field application (*19*). Recently, Pospisil's group reported the influence of β-CD on the reduction mechanism of iprodione in a dimethylsulfoxide solvent (*20*, *21*).

Scheme 1. Chemical Structure of Iprodione

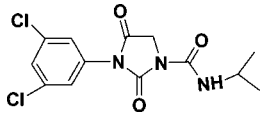

However, there is no report about the bioactivity change upon the formation of the iprodione/β-CD complex.

The aim of this work is to investigate the possibility of obtaining inclusion complexes of iprodione with β-CD, as a first step to obtain formulations that supply a more rational use of this fungicide, improving its water solubility, bioavailability, and fungicidal activity. Additionally, the present work is based on an integrated experimental−computational approach. As compared to the previously used pure experimental approaches, the integrated experimental−computational approach not only demonstrates some macroscopic information about the solubility and possible intermolecular interactions through wet experimental measurements but also provides valuable information about the microscopic binding through the computational modeling.

MATERIALS AND METHODS

Materials and Instruments. All materials were obtained from commercial sources and were used as received unless stated otherwise. Specially, β-CD (≥99%) was obtained from Shanghai Boao Corp. of

* To whom correspondence should be addressed. Tel: +86-27-67867800. Fax: +86-27-68767141. E-mail: gfyang@mail.ccnu.edu.cn.
† Equivalent contributors.

10.1021/jf070197f CCC: $37.00
Published on Web 04/04/2007

China. Iprodione was recrystallized from ethanol and dried at a low temperature. UV spectra were recorded on a UV-2550 (Shimadzu) UV spectrophotometer. Thermogravimetry (TG) and differential scanning calorimetry (DSC) analyses were performed on a Netzsch STA 409 PG/PC instrument with a heating rate of 10 °C/min from 50 to 500 °C. Electrospray ionization mass spectrometry (ESI-MS) experiments were performed on a LCQ ion trap mass spectrometer (Finnigan) equipped with an electrospray ion source.

Preparation and Characterization of Iprodione and β-CD Complex. Iprodione (0.33 g) and β-CD (1.25 g) were completely dissolved in 60 mL of solution of acetone and water (v/v = 1:6). The clear solution was stirred at 60 °C for 3 days. After removal of 30 mL of a acetone−water mixture under vacuum, the reaction mixture was cooled at 2 °C overnight. The precipitate was filtered and washed by a little hot water in order to remove the unreacted β-CD. The obtained residue was dried at 30 °C overnight under high vacuum.

Phase solubility studies were carried out according to Higuchi and Connors's method. An excess amount of iprodione (2 mg) was added to 10 mL of aqueous solutions containing different concentrations of β-CDs (0, 2, 4, 6, 8, 10, 12, and 13 mM). Flasks were sealed to avoid changes due to evaporation, and the solutions were magnetically stirred for a week in a thermostatic bath at 25 °C. After equilibrium was reached, a small volume of the supernatant was withdrawn and filtered through a 0.45 μm hydrophilic membrane filter. The concentration of iprodione in the filtrate was determined by a UV−vis spectrophotometer. The experiments were carried out in triplicate.

The powder X-ray diffraction (XRD) patterns were obtained from a Y-2000 Automatic X-ray diffractometer. The samples were irradiated with monochromatized Cu Kα radiation and mounted on a sample holder and scanned with a step size of 0.03 °C between $2\theta = 5$ and 60 °C. The voltage and current were 30 kV and 20 mA, respectively.

The surface morphology of the raw materials and of inclusion complexes was examined by the field emission scanning electronic microscopy (SEM). These experiments were performed on a JSM-6700F field emission SEM. The samples were fixed on a brass stub using double-sided tape and then gold coated in vacuum by a sutter coater. The pictures were taken at an excitation voltage of 30 kV.

Molecular Modeling. The computations were performed on SGI Fuel workstations and a 128 processor IBM x335 Linux cluster in our lab. The Tripos molecular modeling software package Sybyl 7.0 was used to construct the starting structures of iprodione, β-CD, and possible iprodione/β-CD complexes. The Sander module of Amber 8 program package was used to perform molecular dynamics (MD) simulations on the structures of the free molecules and complexes. The partial atomic charges of iprodione and β-CD required for the MD simulations were calculated by using the RESP protocol implemented in the Antechamber module of the Amber 8 package following electrostatic potential calculations at ab initio HF/6-31G* level with the Gaussian 03 program. The general procedure for carrying out the MD simulations in water was essentially the same as that used in our previously reported other computational studies (*22*−*24*). The MMGBSA (molecular mechanics-generalized Born solvent accessibility) methodology in principle can perform several types of $\Delta G_{binding}$ calculations (enzyme−substrate, protein−protein, and DNA−protein) (*25*−*27*). Basically, MMGBSA calculations predict mean values of interaction free energies as estimated over a series of representative (∼50−100) snapshots extracted from classical MD simulations. The snapshots were post-processed through the removal of all solvent. In this work, a set of 100 representative structures extracted every 10 ps along the (iprodione/β-CD)$_{inside}$ trajectory from 2400 to 3400 ps and a second set of equivalent snapshots extracted every 5 ps from the (iprodione/β-CD)$_{outside}$ trajectory from 2100ps to 2600ps were postprocessed to calculate the binding free energies of (iprodione/β-CD)$_{inside}$ and (iprodione/β-CD)$_{outside}$, respectively, using the MMGBSA approach.

Bioassay. The fungicidal activities of iprodione and the complex against *Rhizoctonia solani* and *Physalospora piricola* in vitro were tested according to our previously reported method (*28*−*30*). The tested samples were dissolved in 0.5 mL of acetone at a concentration of 500 mg/L. The solutions (1 mL) were mixed rapidly with thawed potato glucose agar culture medium (9 mL) under 50 °C. The mixtures were poured into Petri dishes. After the dishes were cooled, the solidified plates were incubated with 4 mm mycelium disk, inverted, and incubated at 28 °C for 48h. The mixed medium without sample was used as the blank control. Three replicates of each test were carried out. The mycelial elongation radius (mm) of fungi settlements was measured after 48 h of culture. The growth inhibition rates were calculated with the following equation: $I = [(C - T)/C] \times 100\%$. Here, I is the growth inhibition rate (%), C is the control settlement radius (mm), and T is the treatment group fungi settlement radius (mm). From a concentration−inhibition ranking ralationship as exemplified in **Figures 1** and **2** for iprodione against *R. solani* and *P. piricola*, respectively, the concentration to give 50% inhibition was defined as EC_{50}.

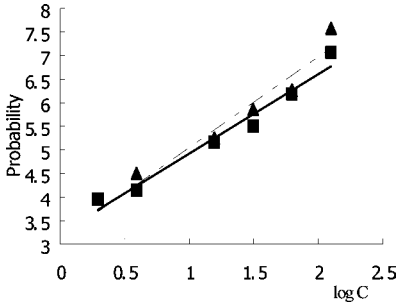

Figure 1. Fungicidal activities of iprodione (▲, $y = 2.1537x + 3.3638$, $EC_{50} = 1.74$ μg mL^{-1}) and iprodione/β-CD complex (■, $y = 1.6805x + 3.2434$, $EC_{50} = 0.76$ μg mL^{-1}) against *R. solani*.

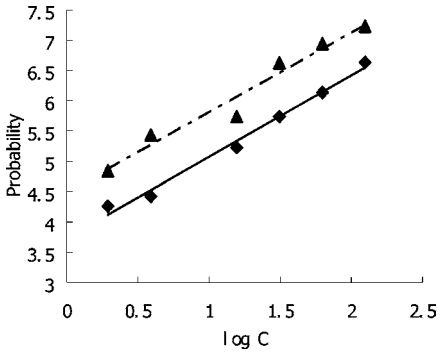

Figure 2. Fungicidal activities of iprodione (▲, $y = 1.6403x + 3.9327$, $EC_{50} = 1.35$ μg mL^{-1}) and iprodione/β-CD complex (■, $y = 1.345x + 3.3707$, $EC_{50} = 0.60$ μg mL^{-1}) against *P. piricola*.

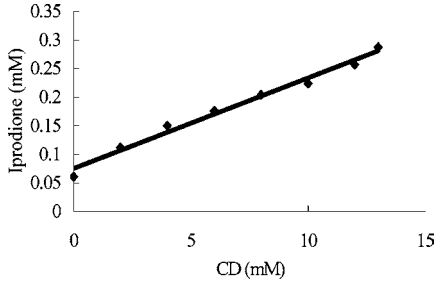

Figure 3. Phase solubility diagram of iprodione in the presence of β-CD.

Bioassay as shown in **Figures 1** and **2** revealed that the EC_{50} values of the inclusion complex against *R. solani* and *Dothiorella gregaria* were 0.76 and 0.60 μM, respectively, whereas the EC_{50} value of iprodione against *R. solani* and *D. gregaria* were 1.74 and 1.35 μM, respectively. This means that the complexation of iprodione with β-CD significantly improved the bioavailability of iprodione due to the improvement of the water solubility.

RESULTS AND DISCUSSION

Phase Solubility and MS Spectrum. The complexation of iprodione and β-CD was evaluated by using the phase solubility method as shown in **Figure 3**. According to Higuchi and Connors (*31*), the phase solubility diagram of iprodione and β-CD is classified as type A_L and indicated the formation of a

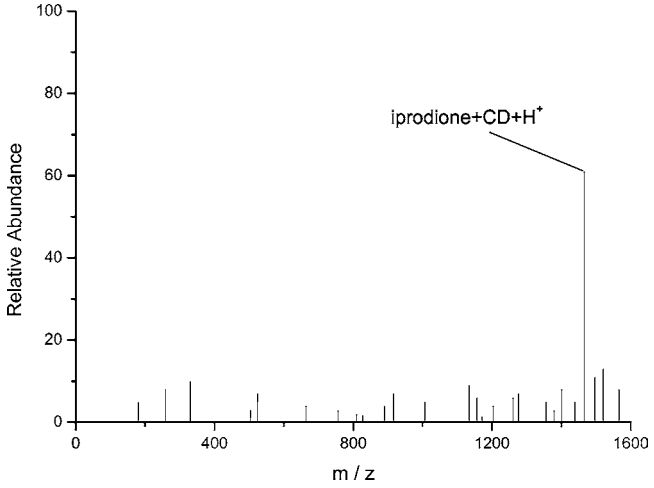

Figure 4. ESI-MS spectrum of the iprodione/β-CD complex.

1:1 inclusion complex between iprodione and β-CD. **Figure 3** shows that the solubility of iprodione increased linearly with increasing concentrations of β-CD. Then, the apparent stability constant, K_c, of iprodione/β-CD complex can be calculated from the slope and the intercept of the linear segment of the phase solubility line, according to the following equation:

$$K_c = k/S_0\,(1 - k)$$

where S_0 is the intrinsic solubility of iprodione in deionized water in the absence of β-CD and k is the slope of the straight line. The calculated apparent stability constant of the iprodione/β-CD complex was 407.5 M^{-1}, which indicated that the interactions between iprodione and β-CD are very strong. As compared with the solubility of iprodione in deionized water in the absence of β-CD, there is a 4.7-fold increase in the presence of 13 mM β-CD.

MS has become a powerful tool for the examination of noncovalent complexes because it is more sensitive as compared to other analytical methods, and most importantly, it provides molecular weight data that allow one to determine the stoichiometry of the complex (*32*−*34*). **Figure 4** illustrates the mass spectra of the inclusion complexes of iprodione with β-CD, from which the most abundant peak observed at *m*/*z* 1467 correspond to [β-CD + iprodione + H]$^+$. These experimental data reveal a dominant host:guest ratio of 1:1 for the iprodione/β-CD inclusion complex in which each iprodione molecule binds with a β-CD molecule.

TG and DSC. A systematic analysis on the TG curves as shown in **Figure 5** indicated that iprodione and β-CD decomposed at 249 and 305.8 °C, respectively. However, the iprodione/β-CD inclusion complexes decomposed at 220.3 °C. The TG curve of the complex indicates that it starts to lose material at a temperature much lower than that of the components, which suggest that the complexation makes the included molecule less stable during heating. When the temperature reached 450 °C, the weights lost of iprodione, β-CD, and the iprodione/β-CD complex are 100, 76, and 97%, respectively. In addition, DSC thermograms provided further information about the thermal property of the iprodione/β-CD complex. As shown in **Figure 6**, iprodione displayed three thermogram endothermic peaks at 132, 276, and 370 °C, and β-CD demonstrated a thermogram endothermic peak at 300 °C. However, the thermogram endothermic peaks of the iprodione/β-CD complex appeared at 125, 275, and 375 °C. Additionally, a broad exothermic peak can be observed around 200 °C.

XRD. Powder X-ray diffractometry is a useful method for the detection of CD complexation in powder or microcrystalline

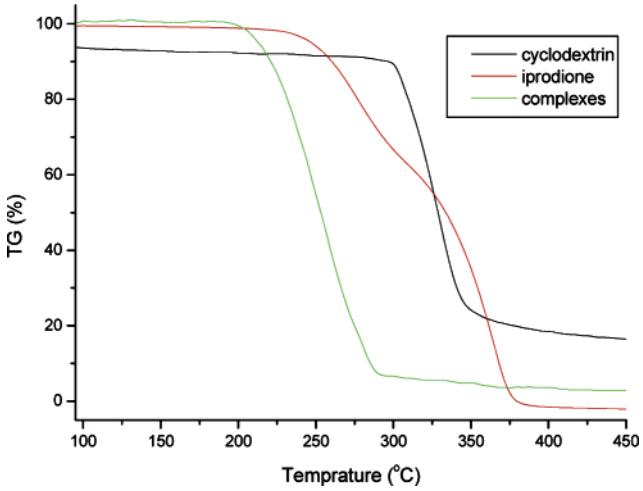

Figure 5. TG thermograms of β-CD, iprodione, and their complex.

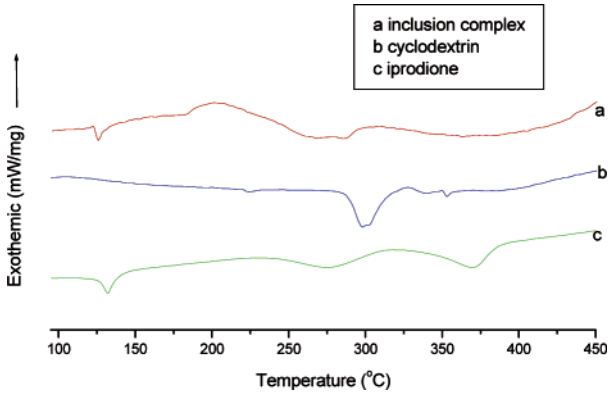

Figure 6. DSC thermograms of β-CD, iprodione, and their complex.

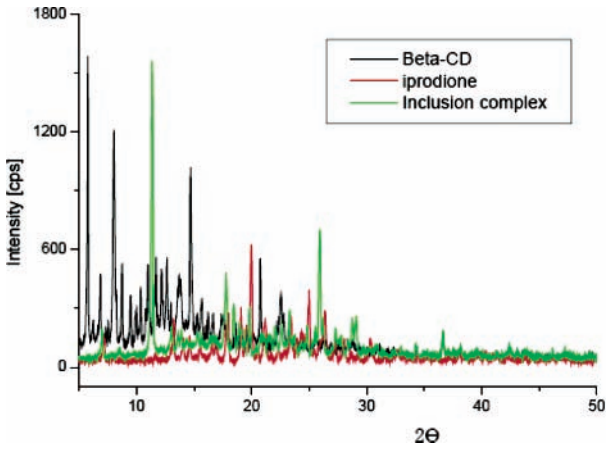

Figure 7. Powder XRD of β-CD, iprodione, and their complex.

states. The diffraction pattern of the complex is supposed to be clearly distinct from that of the superposition of each of the components if a true inclusion complex is formed. As shown in **Figure 7**, some sharp peaks originally in the β-CD sample (e.g., 5.8, 8.0, 14.7, 20.7, and 22.8° 2θ) and in the iprodione sample (e.g., 20.0 and 25.0° 2θ) disappeared, whereas a few new sharp peaks in the complex sample (e.g., 11.3, 17.7, and 26.0° 2θ) appeared, suggesting the formation of the iprodione/β-CD complex.

SEM Images. The surface morphology of the powders derived from iprodione, β-CD, and their inclusion complexes, as assessed by field emission SEM, is provided in **Figure 8**. A comparison of the images revealed that the complex was structurally distinct from the isolated components, those being

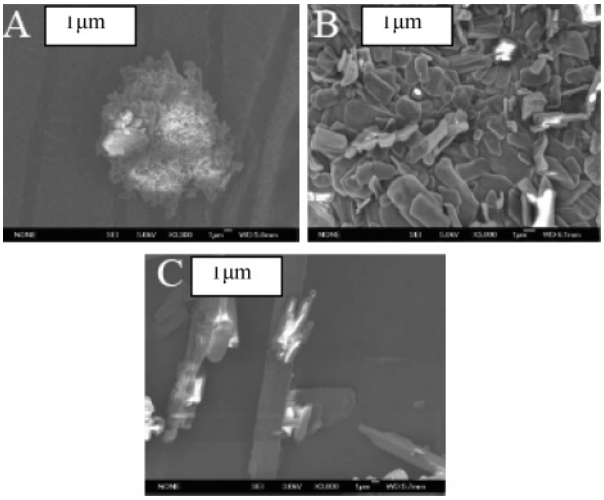

Figure 8. Field emission SEM photographs of (**A**) pure iprodione, (**B**) β-CD, and (**C**) their complex.

the unmanipulated iprodione and β-CD. The sizes and shapes of iprodione and β-CD particles were different from those of the inclusion complex, which confirmed the formation of the inclusion complex.

Proposed Structure of the Iprodione/β-CD Complex by Molecular Modeling. From the above results revealed by phase solubility and MS analysis, we can conclude that a dominant iprodione/β-CD inclusion complex with the stoichiometry of 1:1 was formed. However, we do not know how the iprodione molecule bound with the β-CD molecule. To answer this question, we carried out molecular modeling and MD simulations on various possible microscopic iprodione/β-CD binding modes. Theoretically, there are two possible structures for the iprodione/β-CD inclusion complex with the stoichiometry of 1:1, which were named (iprodione/β-CD)$_{inside}$ and (iprodione/β-CD)$_{outside}$, respectively. In the structure of (iprodione/β-CD)$_{inside}$ as shown in **Figure 9a**, the phenyl group of the iprodione molecule stays inside the hydrophobic cavity of β-CD, with the other side of the iprodione molecule staying outside the cavity on the tail side of the β-CD. In the structure of (iprodione/β-CD)$_{outside}$ as shown in **Figure 9b**, the amino group of the iprodione molecule stays inside the hydrophobic cavity of β-CD, with the phenyl group of the iprodione molecule staying outside the cavity on the tail side of the β-CD.

Figure 10 shows the time dependence of the root-mean-square deviations (rmsd) of the MD-simulated atomic positions of the iprodione/β-CD complexes from the corresponding atomic positions of the energy-minimized structures. These plots are based on the MD simulations in water performed at $T = 298.15$ K and $P = 1$ atm. For each MD simulation, the rmsd values were calculated for the positions of all of the atoms in the simulated complex. As seen in **Figure 10**, the trajectories of the MD simulations on both (iprodione/β-CD)$_{inside}$ and (iprodione/β-CD)$_{outside}$ complexes in water were stabilized during the MD simulations. The MD trajectory was stabilized after ~2400 ps for (iprodione/β-CD)$_{inside}$ and after ~2100 ps for the (iprodione/β-CD)$_{outside}$ complex. After the MD trajectories were stabilized, the average rmsd values were 2.43 Å for the simulated (iprodione/β-CD)$_{inside}$ complex and 2.80 Å for the (iprodione/β-CD)$_{outside}$ complex. These results indicate that the (iprodione/β-CD)$_{inside}$ complex is more stable than the (iprodione/β-CD)$_{outside}$ complex. Furthermore, the MMGBSA model (*23*) was applied to calculate the binding free energy of the (iprodione/β-CD)$_{inside}$ and (iprodione/β-CD)$_{outside}$ complexes. The ΔG values of the (iprodione/β-CD)$_{inside}$ and (iprodione/β-CD)$_{outside}$ complexes are −46.14 and −40.54 kcal/mol, respectively, which

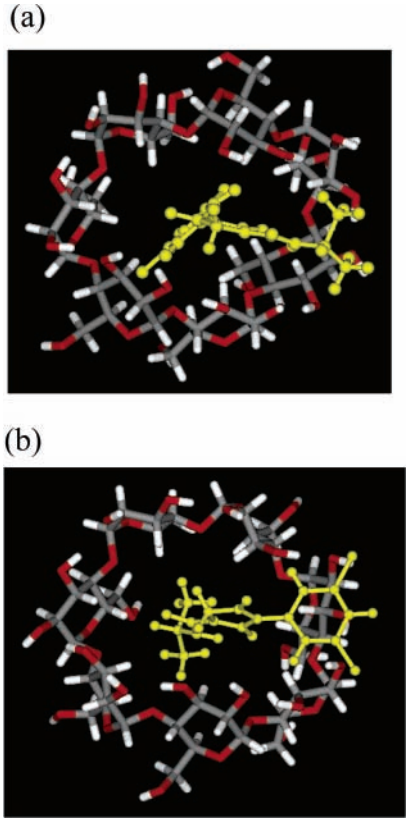

Figure 9. Obtained energy-minimized geometries of two possible iprodione/β-CD inclusion complexes after MD simulation.

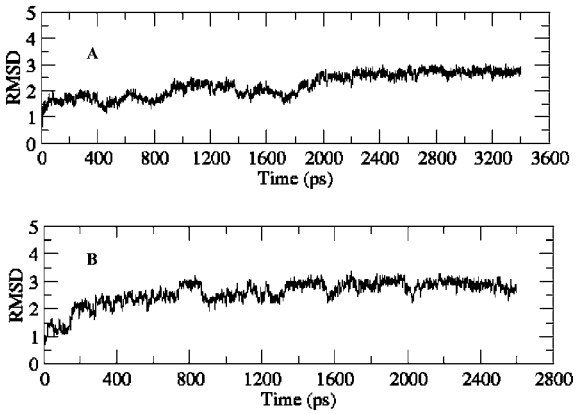

Figure 10. Time dependence of the root-mean-square deviations (rmsd) of atomic positions in the MD-simulated complexes from the (iprodione/β-CD)$_{inside}$ (**A**) and (iprodione/β-CD)$_{outside}$ (**B**) geometries.

indicated that the (iprodione/β-CD)$_{inside}$ complex is much more stable than the (iprodione/β-CD)$_{outside}$ complex, and the hydrophobic binding between the phenyl ring and the inner β-CD cavity might be the main driving force for the formation of the complex.

In summary, extensive experimental data along with computational modeling reveal the formation of a dominant iprodione/β-CD inclusion complex with a stoichiometry of 1:1 through hydrophobic binding. The apparent stability constant of the iprodione/β-CD complex of 407.5 M^{-1} was calculated according to the phase solubility diagram. The complexation of iprodione with β-CD significantly improved the bioavailability of iprodione and, therefore, resulted in over two-fold increase of the fungicidal activity. The significant increase of the bioactivity of iprodione in the presence of β-CD provides an effective approach for a more rational application of iprodione, diminish-

ing the use of organic solvents and the amount of iprodione and increasing its efficacy.

LITERATURE CITED

(1) Szejtli, J. Introduction and general overview of cyclodextrin chemistry. *Chem. Rev.* **1998**, *98*, 1743.

(2) Uekama, K.; Hirayama, F.; Irie, T. Cyclodextrin drug carrier systems. *Chem. Rev.* **1998**, *98*, 2045−2076.

(3) Uekama, K.; Hirayama, F.; Arima, H. Recent aspect of cyclodextrin-based drug delivery system. *J. Inclusion Phenom. Macrocyclic Chem.* **2006**, *56*, 3−8.

(4) Hamada, H.; Ishihara, K.; Masuoka, N.; Nakajima, N. Enhancement of water-solubility and bioactivity of paclitaxel using modified cyclodextrins. *J. Biosci. Bioeng.* **2006**, *102*, 369−371.

(5) Denadai, A. M. L.; Santoro, M. M.; Lopes, M. T. P.; Chenna, A.; de Sousa, F. B.; Avelar, G. M.; Gomes, M. R.; Guzman, F.; Salas, C. E.; Sinisterra, R. D. A supramolecular complex between proteinases and beta-cyclodextrin that preserves enzymatic activity. Physicochemical characterization. *Biodrugs* **2006**, *20*, 283−291.

(6) Balmas, V.; Delogu, G.; Sposito, S.; Rau, D.; Migheli, Q. Use of a complexation of tebuconazole with beta-cyclodextrin for controlling foot and crown rot of durum wheat incited by Fusarium culmorum. *J. Agric. Food Chem.* **2006**, *54*, 480−484.

(7) Villaverde, J.; Maqueda, C.; Morillo, E. Effect of the simultaneous addition of beta-cyclodextrin and the herbicide norflurazon on its adsorption and movement in soils. *J. Agric. Food Chem.* **2006**, *54*, 4766−4772.

(8) Zhang, A. P.; Liu, W. P.; Wang, L. M.; Wen, Y. Z. Characterization of inclusion complexation between fenoxaprop-p-ethyl and cyclodextrin. *J. Agric. Food Chem.* **2005**, *53*, 7193−7197.

(9) Cai, X. Y.; Liu, W. P.; Chen, S. W. Environmental effects of inclusion complexation between methylated β-cyclodextrin and diclofop-methyl. *J. Agric. Food Chem.* **2005**, *53*, 6744−6749.

(10) Villaverde, J.; Maqueda, C.; Morillo, E. Improvement of the desorption of the herbicide norflurazon from soils via complexation with β-cyclodextrin. *J. Agric. Food Chem.* **2005**, *53*, 5366−5372.

(11) Consonni, R.; Recca, T.; Dettori, M. A.; Fabbri, D.; Delogu, G. Structural characterization of imazalil/β-cyclodextrin inclusion complex. *J. Agric. Food Chem.* **2004**, *52*, 1590−1593.

(12) Liu, W. P.; Gan, J. J. Determination of enantiomers of synthetic pyrethroids in water by solid phase microextraction-enantioselective gas chromatography. *J. Agric. Food Chem.* **2004**, *52*, 736−741.

(13) Villaverde, J.; Morillo, E.; Perez-Martinez, J. I.; Gines, J. M.; Maqueda, C. Preparation and characterization of inclusion complex of norflurazon and β-cyclodextrin to improve herbicide formulations. *J. Agric. Food Chem.* **2004**, *52*, 864−869.

(14) Koontz, J. L.; Marcy, J. E. Formation of natamycin: Cyclodextrin inclusion complexes and their characterization. *J. Agric. Food Chem.* **2003**, *51*, 7106−7110.

(15) Orth, A. B.; Sfarra, A.; Pell, E. J.; Tien, M. An investigation into the role of lipid peroxidation in the mode of action of aromatic hydrocarbon and dicarboximide fungicides. *Pestic. Biochem. Biophys.* **1992**, *44*, 91−100.

(16) Ronis, M. J. J.; Badger, T. M. Toxic interaction between fungicides that inhibit ergosterol biosynthesis and phosphorothioate insecticides in the male rat and bobwhite quail (*Colinus virginianus*). *Toxicol. Appl. Pharmacol.* **1995**, *130*, 221−228.

(17) Choi, G. J.; Lee, H. J.; Cho, K. Y. Involvement of catalase and superoxide dismutase in resistance of *Botrytis Cinerea* to dicarboximide fungicide vinclozolin. *Pestic. Biochem. Physiol.* **1997**, *59*, 1−10.

(18) Radice, S.; Ferraris, M.; Marabini, L.; Grande, S.; Chiesara, E. Effect of iprodione, a dicarboximide fungicide, on primary cultured rainbow trout (*Oncorhynchus mykiss*) hepatocytes. *Aquat. Toxicol.* **2001**, *54*, 51−58.

(19) Ma, Z. H.; Michailides, T. J. Characterization of iprodione-resistant *Alternaria* isolates from pistachio in California. *Pestic. Biochem. Phys.* **2004**, *80*, 75−84.

(20) Hromadova, M.; Pospisil, L.; Giannarelli, S.; Fuoco, R.; Colombini, M. P. Electrochemical evidence of host-guest interactions. Changes in the redox mechanism of fungicides iprodione and procymidone in the nano-cavity of cyclodextrins. *Micro-Chem. J.* **2002**, *73*, 213−219.

(21) Hromadova, M.; Pospisil, L.; Zalis, S.; Fanelli, N. Electrochemical detection of host-guest interactions of dicarboximide pesticides with cyclodextrins. *J. Inclusion Phenom. Macrocyclic Chem.* **2002**, *44*, 373−380.

(22) Yang, G. F.; Wang, H. B.; Yang, W. C.; Gao, D. Q.; Zhan, C. G. Formation of supramolecular permethrin/β-cyclodextrin nanorods. *J. Chem. Phys.* **2006**, *125*, 111104.

(23) Zhu, X. L.; Zhang, L.; Chen, Q.; Wan, J.; Yang, G. F. Interactions of aryloxyphenoxypropionic acids with sensitive and resistant acetyl-coenzyme A carboxylase by homology modeling and molecular dynamic simulations. *J. Chem. Inf. Model.* **2006**, *46*, 1819−1826.

(24) Yang, G. F.; Wang, H. B.; Yang, W. C.; Gao, D. Q.; Zhan, C. G. Bioactive permethrin/β-cyclodextrin inclusion complex. *J. Phys. Chem. B* **2006**, *110*, 7044−7048.

(25) Kalra, P.; Reddy, T. V.; Jayaram, B. Free energy component analysis for drug design: A case study of HIV-1 protease-inhibitor binding. *J. Med. Chem.* **2001**, *44*, 4325−4338.

(26) Latha, N.; Jain, T.; Sharma, P.; Jayaram, B. A free energy based computational pathway from chemical templates to lead compounds: A case study of COX-2 inhibitors. *J. Biomol. Struct. Dyn.* **2004**, *21*, 791−804.

(27) Shaikh, S. A.; Ahmed, S. R.; Jayaram, B. A molecular thermodynamic view of DNA-drug interactions: A case study of 25 minor-groove binders. *Arch. Biochem. Biophys.* **2004**, *429*, 81−99.

(28) Huang, W.; Yang, G. F. Microwave-assisted, one-pot syntheses and fungicidal activity of polyfluorinated 2-benzylthiobenzothiazoles. *Bioorg. Med. Chem.* **2006**, *14*, 8280−8285.

(29) Liu, Z. M.; Yang, G. F.; Qing, X. H. Syntheses and biological activities of novel diheterocycle compounds containing 1,2,4-triazolo[1,5-a]pyrimidine and 1,3,4-oxadiazole. *J. Chem. Technol. Biotechnol.* **2001**, *76*, 1154−1158.

(30) Chen, W.; Chen, Q.; Wu, Q. Y.; Yang, G. F. Synthesis and fungicidal evaluation of novel 1,2,4-triazolo[1,5-a]pyrimidine containing oxadiazolyl derivatives. *Chin. J. Org. Chem.* **2005**, *25*, 1477−1481.

(31) Higuchi, T.; Connors, K. A. Phase solubility techniques. In *Advances in Analytical Chemistry Instrumentation*; Reilly, C. N., Ed.; Interscience: New York, 1965; Vol. 4, pp 117−212.

(32) Cuniff, J. B.; Vouros, P. False positives and the detection of cyclodextrin inclusion complexes by electrospray mass spectrometry. *J. Am. Soc. Mass Spectrom.* **1995**, *6*, 437−447.

(33) Guernelli, S.; Laganà, M. F.; Mezzina, E.; Ferroni, F.; Siani, G.; Spinelli, D. Supramolecular complex formation: A study of the interactions between β-cyclodextrin and some different classes of organic compounds by ESI-MS, surface tension measurements, and UV/vis and ^{1}H NMR spectroscopy. *Eur. J. Org. Chem.* **2003**, 4765−4776.

(34) Guo, M.; Song, F.; Liu, Z.; Liu, S. Characterization of noncovalent complexes of rutin with cyclodextrins by electrospray ionization tandem mass spectrometry. *J. Mass Spectrom.* **2004**, *39*, 594−599.

Received for review January 22, 2007. Revised manuscript received February 22, 2007. Accepted February 15, 2007. The present work was supported by National "973" Project (2003CB114400), National NSFC (20572030, 20528201, and 20432010), the Cultivation Fund of the Key Scientific and Technical Innovation Project Ministry of Education of China (705039), and Program for Excellent Research Group of Hubei Province (2004ABC002).

JF070197F